



ISSN: 0067-2904  
GIF: 0.851

## Evaluating the phenomenological approach models in predicting the Neutron Induced Deuteron Emission Spectra from Different reactions

Mahdi Hadi Jasim \*

Department of Physics, college of Science, University of Baghdad

### Abstract

A neutron induced deuteron emission spectra and double differential cross-sections (DDX), in  $^{27}\text{Al} (n, D) ^{26}\text{Mg}$ ,  $^{51}\text{V} (n, D) ^{50}\text{Ti}$ ,  $^{54}\text{Fe} (n, D) ^{53}\text{Mn}$  and  $^{63}\text{Cu} (n, D) ^{62}\text{Ni}$  reactions, have been investigated using the phenomenological approach model of Kalbach. The pre-equilibrium stage of the compound nucleus formation is considered the main pivot in the discription of cross-section, while the equilibrium (pick up or knock out ) process is analyzed in the framework of the statistical theory of cluster reactions, Feshbach, Kerman, and Koonin (FKK) model. To constrain the applicable parameterization as much as possible and to assess the predictive power of these models, the calculated results have been compared with the experimental data and other theoretical work such as TALYS code (Tendl-2014). The comparisons indicate good agreement between these models with the experimental data.

**Keywords:** Neutron induced deuteron emission spectra, Kalbach systematic approach, FKK model, double differential cross-section.

### تقييم نماذج التقريب الظاهري في تنبأ تحريض النيوترون لطيف انبعاث ديتريون ولعدة تفاعلات

مهدي هادي جاسم \*

قسم الفيزياء, كلية العلوم, جامعة بغداد, بغداد, العراق

### الخلاصة

التحقق في تحريض النيوترون لطيف انبعاث ديتريوم وكذلك المقاطع العرضية التفاضلية المزدوجة في التفاعلات  $^{63}\text{Cu} (n, D) ^{62}\text{Ni}$  و  $^{54}\text{Fe} (n, D) ^{53}\text{Mn}$ ,  $^{51}\text{V} (n, D) ^{50}\text{Ti}$ ,  $^{27}\text{Al} (n, D) ^{26}\text{Mg}$ , باستخدام نموذج التقريب الظاهري لكالبخ، لوصف مرحلة التوازن الاولي في تكوين النواة المركبة، بينما عند عملية التوازن (الالتقاط او الأبعاد) تم التحليل باستخدام نظام النظرية الاحصائية للتفاعلات العنقودية، نموذج فيشباخ، كيرمان و كونن. و لغرض حصر المتغيرات قدر الامكان وتحديد قدرة التنبأ لهذه النماذج تم مقارنة البيانات المحسوبة مع البيانات العملية والعمل النظري مثل شفرة تاليس (تندل 2014)، إشارة المقارنة الى تقارب جيد بين هذه النماذج والبيانات العملية.

**Introduction**

An accurate data of energy spectra and double differential cross-sections (DDXs) of neutron-induced charged particle emission becomes an important requirement for the development of Fusion reactor materials. Such development is demonstrating the capacity to produce energy through International Thermonuclear Experimental Reactor (ITER) using deuterium-tritium plasma phase, which represents a flagship project to implement the European strategy for sustainable energy in the future [1,2]. One of the problems normally faced the designer of Fusion Reactor is the continue feeding hydrogen isotopes through the reactions (n, T) and (n, D) and the generation of helium gas through (n, α), and (n, n'α) reactions in the first wall of the blanket material of the reactor. Therefore, by selecting an appropriate blanket material through investigation the energy spectra and DDX distribution of neutron induced hydrogen isotopes, which becomes the necessary condition for the researcher and designer in order to identify the applicable candidate of blanket materials suits the Fusion reactor.

In view of this, and for the necessity enriching the national database [3], the deuteron emission energy spectra and DDX distribution for (n, D) reactions, at different neutron incident energy and target materials, have been carefully calculated in the present work using the Exciton Model (ExM) associated with Feshbach, Kerman, and Koonin (FKK) model. The results are compared with the available TALYS-1.4 code [4] and experimental results.

Many nuclear reactions involve the emission or capture of clusters of nucleons, such as deuterons, Tritons and Helions particles as well as nucleons, are interested in the study of the nuclear structure and nuclear reaction mechanisms. They provide important information on the single particle and on the multi particle character of nuclear states, and so have been widely used as powerful nuclear spectroscopic tools [5].

**Theoretical Model**

The pre-equilibrium spectra could provide information on the cluster emission preformation probabilities in compound nucleus, where the nuclear reaction mechanism comprises the bridge between fast, direct processes, and slow compound processes, and accounts for the high-energy tails in emission spectra and the smooth forward-peaked angular distributions [6,7, 8]. These clusters particles, like deuteron, in pre-equilibrium and compound stages could streamline calculated the energy spectra and DDX distributions in the framework of ExM with FKK model [ 9,10, 11]. Also, the quantum mechanical theories, in the references [12,13,14], have been developed to describe these mechanisms and tend to account for experimental angle integrated emission spectra with higher accuracy comparable to that found in the ExM with FKK model.

In the present calculations the primary pre-equilibrium differential cross section, for the emission of a cluster particle k with emission energy  $E_b$  and can then be expressed in terms of lifetimes  $\tau$  for various classes of stages, with the composite nucleus formation cross section  $\sigma^{CF}$  and an emission rate  $\zeta_b$  in two-component, can be defined as :

$$\frac{d\sigma_b^{pe}}{dE_b} = \sigma^{CF} \sum_{p_\pi=p_\pi^0}^{p_\pi^{max}} \sum_{p_\nu=p_\nu^0}^{p_\nu^{max}} \zeta_b(p_\pi, h_\pi, p_\nu, h_\nu, E^{tot}, E_b, T) \times \tau(p_\pi, h_\pi, p_\nu, h_\nu) \times P(p_\pi, h_\pi, p_\nu, h_\nu) \quad (1)$$

where the factor P represents the part of the pre-equilibrium population that has survived emission.

The basic feeding term for pre-equilibrium emission (PE) is the compound formation cross section  $\sigma^{CF}$ , which is given by:

$$\sigma^{CF} = \sigma_{react} - \sigma_{direct} \quad (2)$$

The reaction cross section  $\sigma_{react}$  is directly obtained from the optical model using the Neutron Spherical Optical-Statistical Model (ABAREX-code system) [15].

The emission rate  $\zeta_b$  has been derived by Cline and Blann [16] from the principle of micro reversibility, and can easily be generalized into a two-component version [17]. The particle b emission rate at the equilibrium stage with relative mass  $\mu_b$ , spin  $s_b$ , isospin quantum number T and the final state isospin  $T_B$  is:

$$\zeta_k(p_\pi, h_\pi, p_\nu, h_\nu, E^{tot}, E_b, T) = \frac{2s_b + 1}{\pi^2 \hbar^3} \mu_b E_b \sigma_{b,inv}(E_b) \times \sum_T (C_b(T, T_B)) \frac{\Omega(p_\pi - Z_k, h_\pi, p_\nu - N_k, h_\nu, E^{tot} - E_b, T_B)}{\Omega(p_\pi, h_\pi, p_\nu, h_\nu, E^{tot}, T)} \quad (3)$$

where  $\sigma_{b,inv}(E_b)$  is the inverse reaction cross section,  $Z_b(N_b)$  is the charge (neutron) number of the ejectile particle b,  $E_{tot}$  is the total energy of the composite system and  $(C_b(T, T_B))$  is the isospin coupling Clebsch-Gorden coefficient for emitted cluster particle b.

For the two-component particle-hole state density,  $\Omega$ , the expression of Betak and Dobes [18, 19] has been used in this work. Their formula is based on the assumption of Eqi-distant Space Model (ESM) and corrected for the effect of the Pauli Exclusion Principle and the Finite depth of the potential well.

**Spectra and angular distributions**

Generally, the pre-equilibrium models ignore the influence of angular momentum. This is easily shown to be rather small for the nucleon emission [20], but is surely greater for clusters. Here, the effect arises from two facts: (i) cluster emission is usually enhanced at higher angular momenta, which means increased role of the nuclear surface and consequently effective lowering of the Coulomb barrier, especially in the case of deformed nuclei [21,22] and (ii) many of the quantities, entering the pre-equilibrium reactions are spin (or both spin and energy) dependent, and their simple contraction to one variable necessarily affects the results.

In nucleon-induced reactions, the original Exciton (in fact, the incident neutron) are presumed to be the most energetic one for the most of the time and as such it keeps the notion of its direction [23], which is slowly smeared out in the course of the reaction. In the energy range of the pre equilibrium models, the nucleon-nucleon differential cross section is nearly isotropic in the C.M. System, so that in the laboratory system, it is proportional to  $\cos \theta$ . The emitted nucleon at the very early stage of the reaction is now just the leading particle, and the angular distribution is that which corresponds to the degree of smearing out the originally sharp value during the time interval from the creation of the composite system to the particle emission.

The original angular distribution formalism divides the cross section into two components, multi-step direct (MSD) and multi-step compound (MSC), following the suggestion of [24]. The MSD cross section is thus assumed to exhibit forward-peaked angular distributions, while the MSC cross section has angular distributions which are symmetric about  $90^\circ$  in the C.M. System [25].

The basic formula for the DDX, that described successfully the shape of the pre-equilibrium angular distributions for the reaction A (a, b) B, using the Kalbach systematic approach [26], and can be written in the following equivalent forms:

$$\frac{d^2\sigma}{d\Omega d\varepsilon_b} = \frac{1}{4\pi} \frac{d\sigma}{d\varepsilon_b} \frac{a_{ex}}{e^{a_{ex}} - e^{-a_{ex}}} \left( (1 + f_{msd}) e^{a_{ex} \cos\theta} + (1 - f_{msd}) e^{-a_{ex} \cos\theta} \right) \quad (6)$$

where  $a_{ex}$  is the slope parameter associated with the ExM and its related components. The quantity  $f_{msd}(\varepsilon_b)$  is the MSD fraction of the cross section at the specified emission energy and it is replaced with the fraction that is pre equilibrium, and the angle  $\theta$  is measured in the C.M. System.

As shown in figure -1 the behavior of the MSD function,  $f_{msd}(\varepsilon_b)$ , of the cross section as a function of emission energy in  $^{232}\text{Th}$  and  $^{209}\text{Bi}$ , with 14.1 MeV, incident neutron, in case of emitted proton and neutron in case of  $^{232}\text{Th}$  and emitted neutron, proton and deuteron in case of  $^{209}\text{Bi}$ .

The MSD spectra or pre equilibrium or forward-peaked component includes the ExM pre equilibrium components, both primary (pre, 1) and secondary (pre, 2) as well as the cross sections from nucleon transfer (NT), knockout and inelastic scattering (IN) involving cluster degrees of freedom. Collective excitations and elastic scattering are treated separately. Thus, for inelastic scattering the energy emission spectrum for cluster b is:

$$\left[ \frac{d\sigma}{d\varepsilon_b} \right]_{MSD} = \left[ \frac{d\sigma}{d\varepsilon_b} \right]_{pre,1} + \left[ \frac{d\sigma}{d\varepsilon_b} \right]_{pre,2} + \left[ \frac{d\sigma}{d\varepsilon_b} \right]_{NT} + \left[ \frac{d\sigma}{d\varepsilon_b} \right]_{IN} \quad (8)$$

The corresponding equilibrium or symmetric component contains only the primary and secondary evaporation cross sections, for primary and secondary emission, and is given by:

$$\left[ \frac{d\sigma}{d\varepsilon_b} \right]_{MSC} = \left[ \frac{d\sigma}{d\varepsilon_b} \right]_{primary-eq.} + \left[ \frac{d\sigma}{d\varepsilon_b} \right]_{secondary-eq.} \quad (10)$$

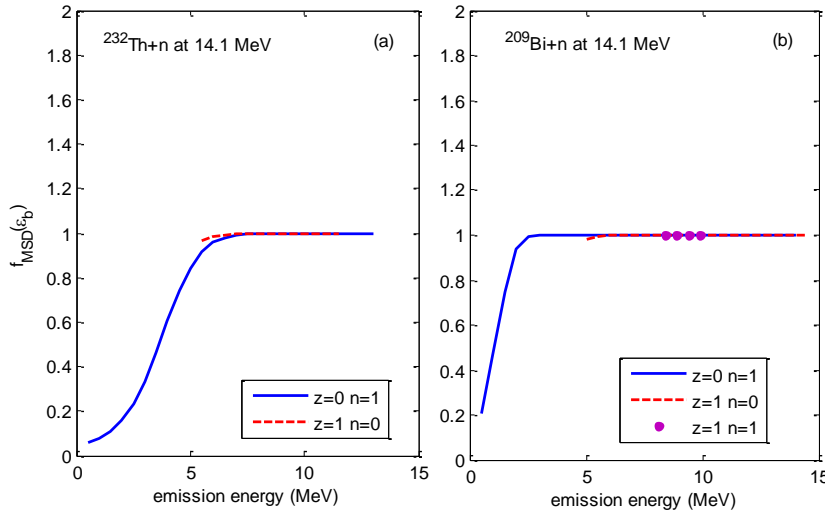


**Figure 1-** Using the FKK model the MSD fraction of the cross section as a function of emission energy in (a) <sup>232</sup>Th and (b) <sup>209</sup>Bi, at 14.1 MeV, incident neutron, in case of emitted proton and neutron for <sup>232</sup>Th and in case of emitted proton, neutron and deuteron for <sup>209</sup>Bi.

**Results and discussions**

The neutron induced deuteron particle emissions in <sup>27</sup>Al (n, D) <sup>26</sup>Mg, <sup>51</sup>V (n, D) <sup>50</sup>Ti, <sup>54</sup>Fe (n, D) <sup>53</sup>Mn and <sup>63</sup>Cu (n, D) <sup>62</sup>Ni reactions have been considered in the present work. The incident neutron energy has been taken in the range 14-15MeV for the necessity demands as the main D-T fusion energy. The calculated data have been compared with the corresponding published experimental data, where the achievement is absolutely acceptable. The figures (2-5) show in general the perfect agreement between present result and Tendl-2012, and experimental data at different neutron energy range (14-15 MeV). By combining the direct, pre equilibrium and compound nuclear models in one calculation one can able to predict the double-differential spectra, figures(6 and 7) and the residual production cross sections of incident energy 14MeV for <sup>27</sup>Al(n, d)<sup>26</sup>Mg and <sup>51</sup>Vl (n, D)<sup>50</sup>Ti reactions, where the maximum deuteron emission energy lied at 4 MeV and 5MeV respectively.

Figure-8 the inter-comparison has been made of the data evaluated in the present work for (n, n) reactions, with the experimentally measured data from EXFOR [30] and with the following theoretical evaluations for (n, n) reactions in references [30, 31, 32, 33, 34].

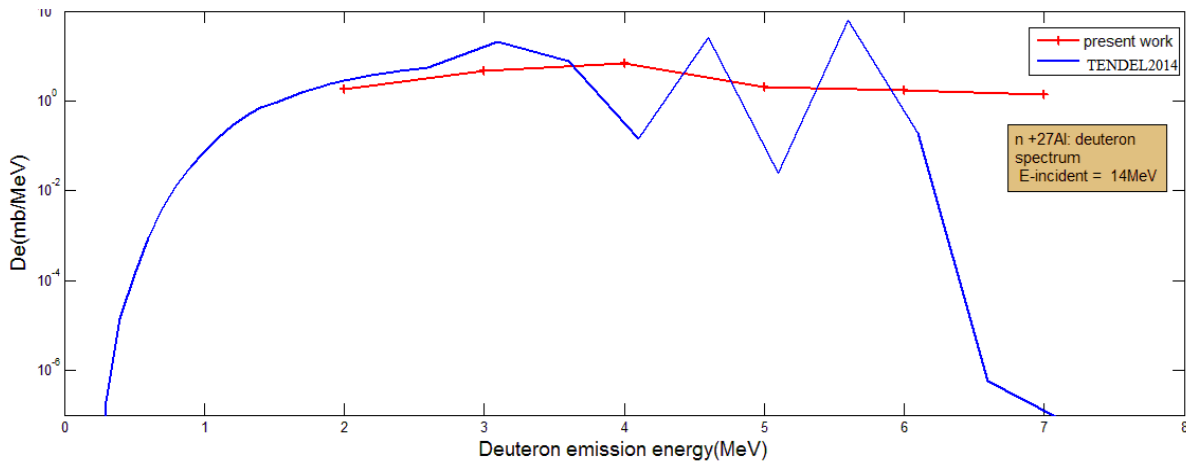


**Figure 2-** the deuteron energy spectra for the reaction <sup>27</sup>Al (n, D) at 14MeV neutrons incident energy compared with ref [27].

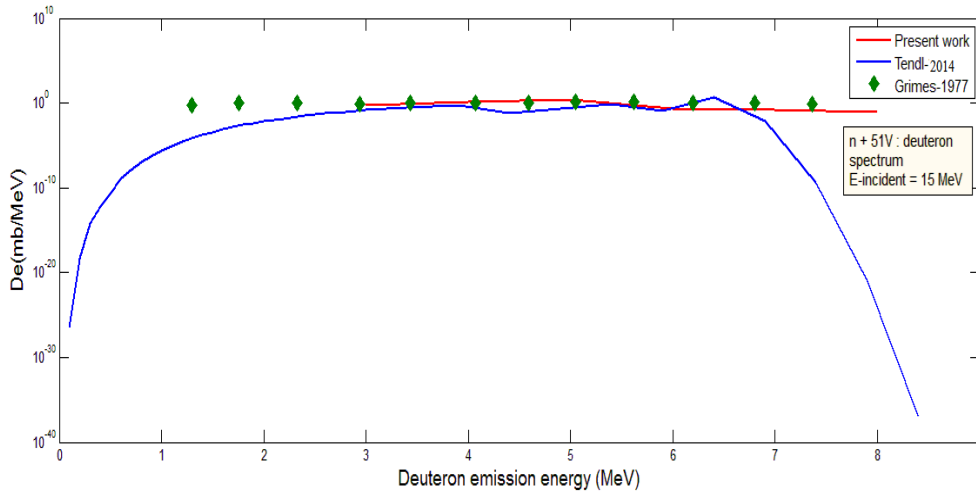


**Figure 3-** the deuteron energy spectra for the reaction  $^{51}\text{V} (n, D)$  at 15MeV neutrons incident energy compared with references [27,28].

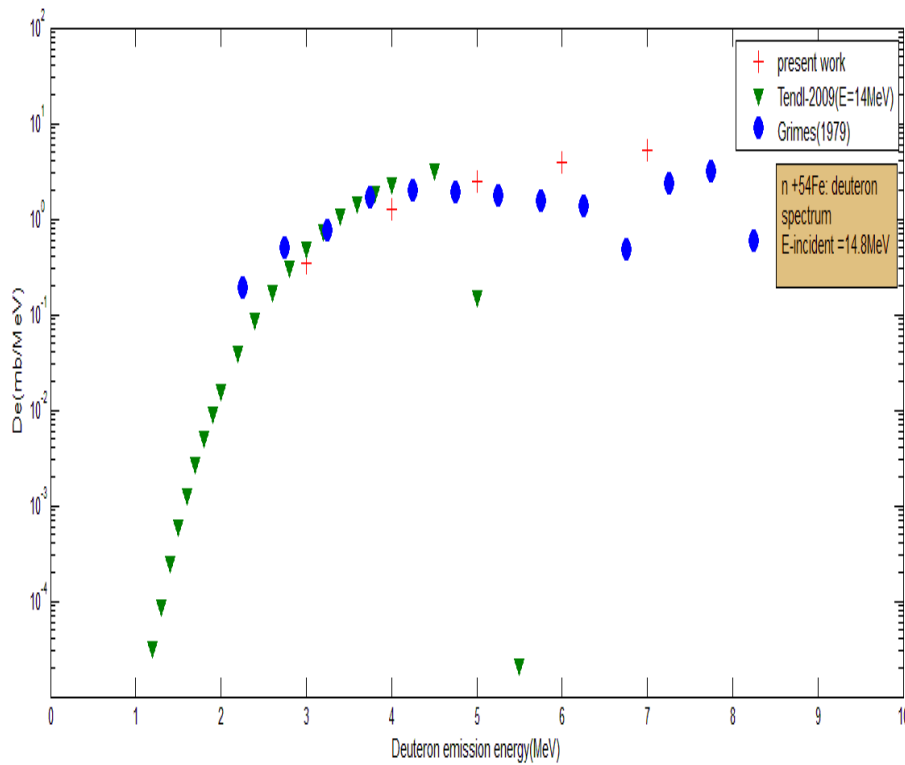


**Figure 4-** the deuteron energy spectra for the reaction  $^{54}\text{Fe} (n, D) ^{53}\text{Mn}$  at 14.8MeV neutrons incident energy compared with references [27, 28].

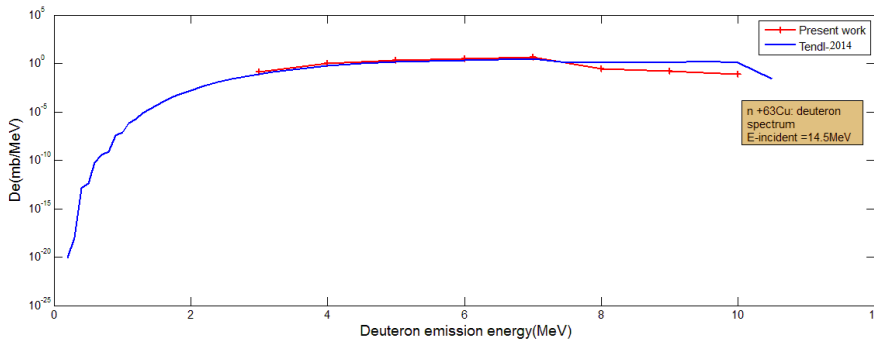


**Figure 5-** the deuteron energy spectra for the reaction  $^{63}\text{Cu} (n, D) ^{62}\text{Ni}$  at 14.5MeV neutrons incident energy compared with ref [27].

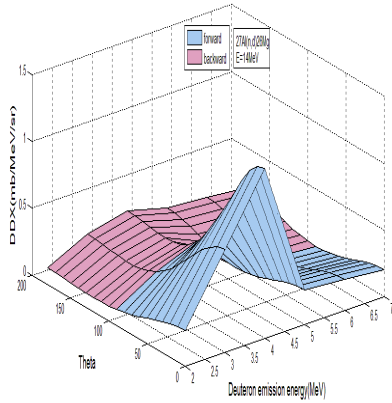


**Figure 6-** The Double Differential Cross-section for the deuteron emission in  $^{27}\text{Al} (n, D) ^{26}\text{Mg}$  reaction at 14 MeV neutron incident energy. Where the probability of deuteron energy around 4 MeV is dominated in the forward direction.

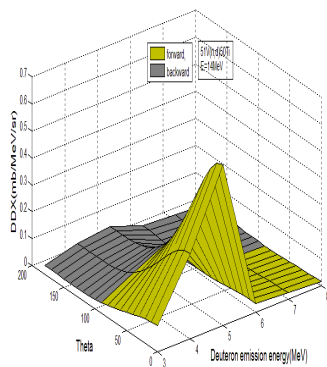


**Figure 7-** The Double Differential Cross-section for the deuteron emission in  $^{51}\text{V} (n, D) ^{50}\text{Ti}$  reaction at 14 MeV neutron incident energy. Where the probability of deuteron energy around 5 MeV is dominated in the forward direction.

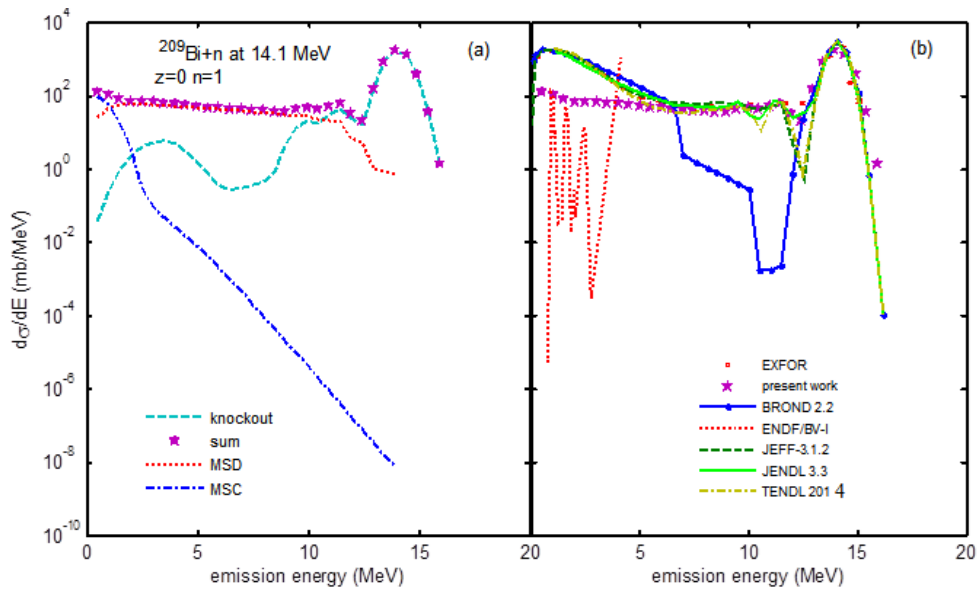


**Figure 8-** A comparison between the energy spectrum calculated in the present work and the experimental data for  $^{209}\text{Bi} (n, n)$  reaction at 14.1 MeV, EXFOR [29], and other theoretical results, (BROND-2.2 [30], ENDF/B-VI [31], JEFF-3.1.2 [32], JENDL-3.3 [33], TENDL -2014 [34]).

## Conclusion

In the present work the phenomenological approach model of Kalbach by extending the formalism to include the MSD and MSC parts of the statistical theory of cluster reactions, FKK model, have used to calculate and analyze the neutron induced deuteron emission spectra and DDX in  $^{27}\text{Al}$ ,  $^{51}\text{Vi}$ ,  $^{54}\text{Fe}$  and  $^{63}\text{Cu}$  nuclei in the neutron energy range 14-15 MeV. The descriptions of spectra improved by including the forward peak, MSD, fraction,  $f_{msd}(\epsilon_b)$ , to the pre equilibrium components, for both primary and secondary, as well as the spectra from nucleon transfer, knockout and inelastic scattering, which involved cluster degrees of freedom. The predictive power of this analysis is the capability to diagnose and constrain, successfully, the applicable parameterization as much as possible for the deuteron emission energy, especially when we obtained the acceptable comparisons with the experimental works of Grimes [28], figures (4) for  $^{54}\text{Fe}(n, D)^{53}\text{Mn}$  at 14.8MeV neutrons incident energy, and other theoretical work of TALYS code (TENDL-2012) [27], figures (2, 3, and 5) for  $^{27}\text{Al}$ ,  $^{51}\text{Vi}$  and  $^{63}\text{Cu}$  nuclei respectively. The behavior of the DDX distributions indicates the maximum deuteron emission is found at 4 MeV in  $^{27}\text{Al}(n, D)^{26}\text{Mg}$  reaction, figure (6), and 5MeV in  $^{51}\text{Vi}(n, D)^{50}\text{Ti}$  reaction, figure (7), at 14 MeV neutron incident energy. Also, the present method examines the behavior of  $^{209}\text{Bi}(n, n)$  energy spectrum at 14.1 MeV, and compared with the available experimental data and theoretical master codes. It shows an acceptable agreement with EXFOR [29], ENDF/B-VI [31], JENDL-3.3 [33] and TENDL -2011 [34], and disagree with the evaluation data for BROND-2.2 [30] and JEFF-3.1.2 [32].

## References:

1. Summary of the ITER final report .2001. *ITER EDA Document* series no.22, IAEA, Vienna.
2. Lalremruata, B. , Dhole, S.D. , Ganesan, S. ,Bhoraskar, V.N. 2009. Double Differential Cross-section of (n, $\alpha$ ) reactions in aluminum and nickel at 14.77 MeV neutrons. *Nucl. Phys. A* 821(1-4), pp:23-25.
3. McLane, V. Rev. 2000 . EXFOR Basics: A Short Guide to the Nuclear Reaction Data Exchange Format, Brookhaven National Laboratory report *BNL-NDC-63380*.
4. Kalbach, C. 1988. Systematics of Continuum Angular Distributions: Extensions to Higher Energies. *Phys. Rev. C* 37, 2350-2370.
5. Hodgson, P. E. and Betak, E. 2003. Cluster emission, transfer and capture in nuclear reactions. *Physics Reports* 374 pp:1-89.
6. Dityuk, A. I., Konobeyev, A.Yu., Lunev, V.P., Shubin, Yu. N. 1997. New Advanced Version of Computer Code ALICE – IPPE. *INDC(CCP)-410*.
7. Koning, A. J. , Chadwick, M. B. 1997. Microscopic two-component multistep direct theory for continuum nuclear reactions. *Phys. Rev. C* .Volume 56,number 2.pp:970.
8. Gadioli, E. and Hodgson, P.E. 1992. *Pre-equilibrium Reactions*. Clarendon Press. Oxford studies in Nuclear Physics.
9. Bonetti, R. Chadwick, M. B. Hodgson, P. E. Carlson, B.V. and Hussein, M.S. 1991. The Feshbach, Kerman, and Koonin Multistep compound Reaction Theory. *Phys. Rep.* 202(4). Pp: 171-231.
10. Bonetti, R. Koning, A.J. Akkermans, J.M. and Hodgson, P.E. 1994. The Feshbach, Kerman, and Koonin Multistep Direct Reaction Theory. *Phys. Rep.* 247(1). Pp: 1-58.
11. Koning, A. J. Hilaire, S. and Goriely, S. 2011. Talys User Manual, A nuclear reaction program, Nuclear Research and Consultancy Group (NRG) Westerduinweg, *NL-1755 ZG*, Petten, The Netherlands.
12. Koning, A.J. and . Duijvestijn, M.C. 2004. A global pre-equilibrium analysis from 7 to 200 MeV based on the optical potential. *Nucl. Phys. A*744 15-76.
13. Chadwick, M.B. Oblozinsky, P. Hodgson, P.E. and Reffo, G. 1991. Pauli-blocking in the quasideuteron model of photoabsorption. *Phys. Rev.* Vol. C44. – PP: 814 – 823; Handbook on photonuclear data for applications: Cross sections and spectra. 2000. *IAEA-TECDOC-1178*.
14. Gruppelaar, H. . Nagel, Pand Hodgson, P.E. 1986. Pre-equilibrium processes in nuclear reaction theory: the state of the art and beyond. *La Rivista Del Nuovo Cimento*, 9 (7): pp:1-46.

15. Lawson, R.D. and Smith, A. B. **1999**. A Neutron Spherical Optical- Statistical- Model Code- A User's Manual ABAREX. *ANL/NDM-145*; Lawson, R.D. and Smith, A. B. **1999**. Elemental ABAREX, A User's Manual Rev. I. *ANL/NDM-147*.
16. Cline, C.K. and Blann, M. **1971**. The pre-equilibrium statistical model: Description of the nuclear equilibration process and parameterization of the model. *Nucl. Phys.* A172, pp:225.
17. Dobes, J. and Betak, E. **1983**. Two-component exciton mode. *Zeit. Phys.* A310, pp:329.
18. Dobes, J. and Betak, E. **1976**. The finite depth of the nuclear potential well in the exciton model of pre-equilibrium decay. *Zeit. Phys.* A279, pp: 319.
19. Fu, C.Y. **1984**. Paring correction of particle-hole state densities for two kinds of fermions. *Nucl. Sci. Eng.* 86, pp: 344.
20. Betak, E. **1995**. Rule of Spin in pre equilibrium calculations. *Acta Phys. Slov.* 45, pp: 625.
21. Blann, M. **1971**. Hybrid Model For Pre-Equilibrium Decay in Nuclear Reactions. *Phys. Lett. B* 27, pp: 27.
22. Blann, M. and Komoto ,T.T. **1981**. Cluster Emission Amplification from nuclei at high angular momenta. *Phys. Rev. C* 24, pp:426.
23. Betak, E. **2002**. *Pre-Equilibrium Complex Particle Emission. Nuclear Theory*. 21ed. V. Nikolaev, Heron Press, Sofia.
24. Feshbach, H. Kerman, A. and Koonin, S. **1980**. *Ann. Phys. (N.Y.)* 125. pp: 429.
25. Kalbach, C. **2006**. *USERS MANUAL for PRECO*. Duke University.
26. Kalbach, C. **1988**. *Phys. Rev. C* 37, pp: 2350.
27. Koning, A.J. and Rochman, D. **2012**. *Talys Tendl-2012*, Nuclear Research and Consultancy Group (NRG) Petten-. Netherland.
28. Grimes, S.M. Haight, R.C. Alvar, K.R. Barschall, H.H. and Borchers, R.R. **1979**. Charged Particle Emission in Reactions of 15 MeV Neutrons with Isotopes of Chromium, Iron, Nickel and Copper. *Phys.Rev.* C19. p.2127.
29. Baba, M. EXFOR, M.Baba, Wakabayashi, H., Itoh,N., Maeda,N., Hirakawa, K., N. R. **1989**. *INDC(JPN)-129*.
30. Nikolaev, M. N. Manturov, G. N. Kostcheev, W.N. **1983**. BROND-2.2. EVAL-NOV83, J., YK, V.1, PP:50.
31. Herman, M. and Trkov, A. **2009**. ENDF-6 Formats Manual Data Formats and Procedures for the Evaluated Nuclear Data File ENDF/B-VI and ENDF/B-VII. *Report BNL-90365*.
32. Maslov, V.M. Porodzinskij, Yu.V. Baba, M. Hasegawa, A. Kornilov, N.V. Kagalenko, A.B. and Teterova, N.A. **2001**. *JEFF-3.1.2. EVAL Neutron Data. NEA-IAEA*.
33. Ohsawa, T. **2001**. *JENDL-3.3 Neutron Data Eval. NEA-IAEA*.
34. Koning, A.J. and Rochman, D. **2011**. *TENDL Neutron Data EVAL-NOV. NEA-IAEA*.